

Journal of Materials Chemistry A

Accepted Manuscript



This is an *Accepted Manuscript*, which has been through the Royal Society of Chemistry peer review process and has been accepted for publication.

Accepted Manuscripts are published online shortly after acceptance, before technical editing, formatting and proof reading. Using this free service, authors can make their results available to the community, in citable form, before we publish the edited article. We will replace this *Accepted Manuscript* with the edited and formatted *Advance Article* as soon as it is available.

You can find more information about *Accepted Manuscripts* in the [Information for Authors](#).

Please note that technical editing may introduce minor changes to the text and/or graphics, which may alter content. The journal's standard [Terms & Conditions](#) and the [Ethical guidelines](#) still apply. In no event shall the Royal Society of Chemistry be held responsible for any errors or omissions in this *Accepted Manuscript* or any consequences arising from the use of any information it contains.

Fabrication of Ordered Mesoporous Carbon Hollow Fiber Membranes via a Confined Soft Templating Approach

Jiansheng Li, Junwen Qi, Chao Liu, Liang Zhou, Hao Song, Chengzhong Yu*, Jinyou Shen, Xiuyun Sun, Lianjun Wang*

[*] Prof. J.S. Li, J.W. Qi, C. Liu, J.Y. Shen, X.Y. Sun, Prof. L.J. Wang

Jiangsu Key Laboratory of Chemical Pollution Control and Resources Reuse

School of Environmental and Biological Engineering

Nanjing University of Science and Technology

Nanjing 210094, P.R. China

E-mail: wanglj@njjust.edu.cn

Dr. L. Zhou, H. Song, Prof. C.Z. Yu

Australian Institute for Bioengineering and Nanotechnology, The University of Queensland

Brisbane, QLD 4072, Australia

E-mail: c.yu@uq.edu.au

Abstract: Ordered mesoporous carbon (OMC) membranes have broad applications such as size exclusive separation of molecules. In this work, a new method to prepare OMC hollow fiber membranes through a confined soft templating route is developed. In this method, commercialized polymeric hollow fiber ultrafiltration membranes were immersed in an ethanol solution containing phenolic resin and Pluronic triblock copolymer. Upon solvent evaporation, the phenolic resin and surfactant self-assembled in the confined voids of the ultrafiltration membrane. After drying and pyrolysis, OMC hollow fiber membranes were obtained. The OMC hollow fiber membranes possess continuous membrane walls with an average thickness of 113 μm . The membrane wall has a hierarchical pore structure: one coming from hexagonally ordered mesoporous carbon with a pore diameter of ~ 4.3 nm, the other being disordered defect holes with a size of 8-50 nm randomly distributed inside the OMC matrix. The gas permeance results indicate that the OMC hollow fiber membranes exhibit Knudsen diffusion behavior confirming the good quality of the membrane.

Keywords: Ordered mesoporous carbon; hollow fiber membranes; soft templating; gas permeation

1. Introduction

Carbon membranes have attracted considerable attention over the past decades due to their advantages such as high thermal, chemical stability and broad applications¹⁻³. Although microporous carbon molecular sieve membranes have been extensively investigated, the reports on the synthesis and application of mesoporous carbon membranes are still limited⁴. The synthesis of ordered mesoporous carbon (OMC) materials was firstly reported by Ryoo and co-workers using ordered mesoporous silica as hard templates⁵. However, it is difficult to prepare OMC membrane using the hard templating approach. Recently, a soft templating method has been developed for the synthesis of OMC materials using phenolic resins as carbon precursors and block copolymers as templates⁶⁻⁹. This method enables the generation of OMC with various morphologies by finely controlling the self-assembly of phenolic resin and block copolymer. Particularly, self-standing OMC membranes⁴ and supported OMC membranes on different substrates (such as anodic alumina^{10,11} and porous ceramic tube¹²) have been successfully prepared.

The hollow fiber morphology is a preferred geometry in industrial-scale applications because of the high packing density and easy module assembly¹³. Compared to their polymeric counterparts, carbon hollow fiber membranes have improved mechanical and chemical stability¹⁴. Recently, strong interest has been shown in the preparation of microporous carbon molecular sieve hollow fiber membranes¹³⁻¹⁹. However, there is no report on the preparation of OMC hollow fiber membranes.

Herein, for the first time, we report the synthesis of OMC hollow fiber membranes through a confined soft-templating method. The preparation of the OMC hollow fiber membranes relies on

the impregnation of precursor solution containing phenolic resin and amphiphilic triblock copolymer (PluronicF127) into the voids of commercially available polymeric ultrafiltration membranes. Upon solvent evaporation, phenolic resin and surfactant self-assembled into ordered mesostructures within the polymeric membrane. After drying and pyrolysis, mesoporous carbon hollow fiber membranes were obtained. The quality of the synthesized OMC hollow fiber membranes were evaluated by gas permeation, showing good potential in gas separation applications.

2. Experimental

2.1. Chemicals and materials

Poly(propylene oxide)-block-poly(ethylene oxide)-block-poly(propylene oxide) type triblock copolymer Pluronic F127 ($\text{PEO}_{106}\text{PPO}_{70}\text{PEO}_{106}$, M_w of 12,600) was purchased from Sigma-Aldrich Corp. Phenol, formalin solution (37 wt %), NaOH, HCl, and ethanol were purchased from Shanghai Chemical Corp. The Polyvinylidene Fluoride (PVDF) ultrafiltration hollow fiber membranes with an average pore size of $\sim 0.1\mu\text{m}$ were purchased from Tianjin Motian Membrane Technology Co., Ltd. All chemicals were used as received without any further purification. Millipore water was used in all experiments.

2.2 Preparation of resol precursors

The phenolic resol precursor was prepared according to a literature method¹⁹. In a typical procedure, 0.61 g of phenol was melted at 40-42°C in a flask and mixed with 0.13 g of 20 wt % NaOH aqueous solution under stirring. After 10 min, 1.05 g of formalin (37 wt % formaldehyde) was added dropwise below 50 °C. Upon further stirring for 1 h at 70-75 °C, the mixture was cooled to room temperature and the pH value was adjusted to about 7.0 by HCl solution. After

water was removed by vacuum evaporation below 50 °C, the final product was dissolved in ethanol (20 wt % ethanolic solution).

2.3 Synthesis of OMC hollow fiber membranes

The OMC hollow fiber membranes were prepared by the self-assembly of resols and triblock copolymer F127 templates in the pores of PVDF ultrafiltration hollow fiber membranes. The process of confined soft-templating approach is schematically illustrated in Fig.1. In a typical preparation, 3.2 g of triblock copolymer F127 was dissolved in 16.0 g of ethanol and 2.0 g of 0.2 M HCl. The mixture was stirred for 1 h at 40 °C to give a clear solution. Next, 10.0 g of 20 wt % precursor solution was added. After being stirred for 2 h, the mixture was transferred into a Petri-dish with a diameter of 12cm. Subsequently, PVDF ultrafiltration hollow fibers with a length of 10 cm were soaked in the mixture. It took 8 h at room temperature to evaporate the ethanol. After the prescribed time elapsed, the residual sol in the lumen of PVDF fibers was removed carefully. The residual sol in the Petri dish was used to prepare unsupported membranes. The impregnated PVDF hollow fibers and the unsupported membranes were dried at 100 °C for 12 h. The unsupported membrane was carefully peeled off from glass dishes and pyrolyzed along with soaked fibers in a tubular furnace at 350 °C for 2 h and then at 700°C for 3 h under N₂ flow at a heating and cooling rate of 1°C min⁻¹.

2.3. Characterization

A thermogravimetric analyzer (TGA) from TA Instruments (model Q600) was used to characterize the weight loss of the pure PVDF hollow fiber membranes, OMC precursor, and the impregnated hollow fiber membrane. The content of OMC (C_{OMC}) was calculated by the following equation: $C_{OMC} = \frac{(W_{\text{impregnated fiber}} - W_{\text{pvdf}}) \cdot R_{\text{omc}}}{W_{\text{impregnated fiber}} \cdot R_{\text{impregnated fiber}}}$, where $W_{\text{impregnated fiber}}$ is the initial

weight of impregnated hollow fiber membranes, W_{pvdf} is the initial weight of PVDF hollow fiber membrane, R_{omc} is the weight loss of unsupported OMC membrane, $R_{\text{impregnated fiber}}$ is the weight loss of impregnated hollow fiber membranes.

Scanning electron microscopy (SEM) observation was performed on a JEOL JSM-6380LV and JSM-7800F electron microscope. The unsupported OMC membrane and OMC hollow fiber membrane after pyrolysis were ground into powders for X-ray diffraction (XRD) characterization, which was performed on a Bruker D8 diffractometer using Cu K α radiation with a step size of 0.02 $^{\circ}$ s at 40 kV and 40 mA. Transmission electron microscopy (TEM) study was carried out using a JEOL JEM-2010 electron microscope operated at 200 kV. The N₂ adsorption-desorption isotherms were measured by a Micromeritics ASAP-2020 analyzer at liquid nitrogen temperature (77K). The specific surface areas were evaluated using the Brunauer-Emmett-Teller (BET) method. A single OMC hollow fiber membrane with a length of 7 cm was constructed by 1/4 inch stainless steel tube, Swagelok tees and unions. The gas permeation measurements for OMC hollow fibers were carried out using pure gas of hydrogen, helium, nitrogen, argon and carbon dioxide. The feed side of the membrane was maintained at a constant pressure in the range of 100-160 kPa. The permeation side of the membrane was set at the atmospheric pressure. The flow rate of gas through the membrane was tested at room temperature with a soap flow meter.

3. Results and discussion

3.1 Morphology of OMC hollow fiber membranes

Fig. 2 is the digital photo of the PVDF hollow fiber membrane, impregnated hollow fiber membrane and OMC hollow fiber membrane. The commercial PVDF hollow fiber membrane used in our synthesis has an outer diameter is about 1 mm (Fig. 2a). After the impregnation of

phenolic resol and triblock copolymer, the color changes from white to yellowish (Fig.2b). After the pyrolysis at 700 °C, black OMC hollow fiber membrane can be obtained with apparent shrinkage in diameter (Fig.2c). However, the intact hollow fiber membrane morphology is reserved.

Representative SEM images of PVDF hollow fiber membranes, impregnated and pyrolyzed hollow fiber membranes are shown in Fig. 3 to illustrate the changes in morphology during the synthesis procedures. From the cross-section SEM images of PVDF hollow fiber membranes, the hollow morphology can be clearly seen and the thickness of PVDF membrane walls is estimated to be 170 μm (Fig. 3a, see Table 1). At the outer edge in the cross section of PVDF fiber, densely packed radial pore channels can be observed. The majority of the polymeric membrane has a highly porous sponge-like structure as shown in Fig.3b. After the impregnation of phenolic resol and triblock copolymer template, only a fraction of the radial pore channels were filled (Fig. 3c); however, the original porous voids in the sponge-like structure were almost fully impregnated (Fig.3d) due to its relatively smaller voids size compared to the radial pore channels located at the outer edge.

In order to elucidate the mesoporous structure of the OMC hollow fiber membranes, field emission SEM (FE-SEM) analysis was used. As shown in Figs.3e, the thickness of the membrane walls is reduced to 113 μm due to the thermal shrinkage in the high temperature pyrolysis process. The unfilled radial pore channels can also be observed at the outer edge in the cross section of the pyrolyzed fiber, in agreement with the impregnated fiber (Fig. 3c). The membrane wall after pyrolysis is dense and continuous. Interestingly, stripe-like arrays can be observed under high magnification (Fig. 3f), indicating that the membrane wall is composed of ordered

mesostructured domains. These ordered domains distributed randomly in the whole area of Fig. 3f. The choice of parent PVDF polymeric membranes with macroporous sponge-like structure plays an important role in the successful synthesis of OMC fiber membrane. The ordered regions are derived from the confined self-assembly of phenolic resin and triblock copolymer template (F127) in the sponge-like macropores of the polymeric membranes. The FESEM results provide a direct evidence of the formation of ordered mesostructure in the hollow fiber carbon membrane.

The dimension changes of PVDF hollow fiber membranes, impregnated and pyrolyzed hollow fiber membranes are summarized in Table 1 based on the SEM observations. Clearly, after pyrolysis, the OMC fiber showed similar shrinkage ratio in the radial (30.0% for outer diameter and 28.0% for inner diameter) and axial directions (31.0%) compared to the original PVDF hollow fiber. The consistent shrinkage in both radial and axial directions indicates an isotropic thermal decomposition behavior during the pyrolysis procedure.

3.2 Structure of OMC hollow fiber membranes

The weight loss measurement for the pyrolysis process was carried out using TGA to mimic the carbonization conditions and hence assess the weight changes of the precursors as a function of temperature during the carbonization process. As shown in Fig. 4, a huge weight loss can be observed for unsupported OMC membrane (57.6%) and impregnated fiber (50.9%) before 350°C. However, only 9.2% weight loss was occurred before 350°C for pure PVDF hollow fiber. The tremendous difference is due to the different decomposition temperature between template F127 (200-370 °C)²¹ and PVDF (above 423°C)²². After final pyrolysis at 700°C, the weight loss for PVDF hollow fiber membrane, impregnated hollow fiber membranes, and unsupported OMC membrane is 69.7%, 71.1%, and 74.1%, respectively. Based on the TGA data, that is the weight

change of PVDF hollow fiber membrane before and after impregnation of phenolic resin, the content of ordered mesoporous carbon in the final hollow fiber carbon membrane is determined to be 69.8%.

Fig. 5 shows the small-angle XRD patterns of the unsupported OMC membrane and OMC hollow fiber membrane after pyrolysis at 700°C for 3 h. The unsupported OMC membrane exhibits two sharp diffraction peaks at 2θ of 0.95 and 1.67°. A peak with weak intensity is also observed at 2θ of $\sim 1.90^\circ$ as indicated by an arrow in the inset of Fig. 5. The three peaks can be indexed as the 100, 110, and 200 diffractions of a hexagonal mesostructure (space group of $p6mm$)^{23,24}. For the OMC hollow fiber membrane, the observed diffraction peaks shift to lower angles. The 100 diffraction appears at 2θ of 0.85°. The unit cell parameter of OMC hollow fiber membrane is calculated to be 11.96 nm, larger than that of unsupported OMC membrane (10.73 nm). This result suggests that the thermal shrinkage of self-assembled phenolic resin and triblock copolymer composites confined within the PVDF voids is much less compared to that of the unsupported membrane. It is proposed that the strong surface interaction between the PVDF walls with the phenolic resin precursor may generate stretching effect during the pyrolysis, leading to reduced shrinkage in the OMC fiber membrane. Similar results were observed in confined assembly of OMC in AAO template^{25,26}.

A more detailed structural characterization is revealed by TEM images, as shown in Fig. 6. The unsupported OMC membrane shows large areas of ordered stripe-like domains, indicating the highly ordered mesostructure (Figs. 6a,b). The image taken from the [100] direction together with the corresponding FFT diffractogram further confirms a 2-D hexagonal ($p6mm$) symmetry. For the OMC hollow fiber membrane, ordered mesostructure can also be observed. However, the

stripe-like mesostructure arranged randomly, which is confirmed by the corresponding FFT diffractogram (Fig.6c). It is worth noticing that there are extensive structural defect holes amid the mesochannels. These holes are irregular in shape with a size of 8-50 nm. The presence of such holes with large pore sizes inside the membrane facilitates the diffusion of molecules inside the OMC structure, which is highly important for membrane applications. Fig.6d is a TEM image at a higher magnification from the marked area in Fig.6c. This image illustrates the coexistence of stripe-like structure and hexagonally arrayed pores in the adjacent area. The TEM results are in well agreement with the FESEM observations (Fig. 3f). Estimated from TEM images, the cell parameters (a_0) are 10.8 and 12.0 nm for the unsupported OMC membrane and OMC hollow fiber membrane, respectively, in accordance with the values calculated from XRD data.

Fig. 7 shows the N_2 adsorption isotherms and pore size distribution of the unsupported OMC membrane and OMC hollow fiber membrane. The unsupported OMC membrane shows a typical type IV isotherm with an obvious H1-type hysteresis loop (Fig.7a). A capillary condensation step occurs at the relative pressure of $P/P_0=0.4-0.7$, characteristic of a mesoporous structure²⁷. The OMC hollow fiber sample shows a H4-type hysteresis loop, in accordance with its structure, i.e., there are disordered voids with large size randomly distributed in the OMC matrix with relatively small pore sizes (4.33 nm, see below)²⁸.

The pore size distribution curves calculated from the adsorption branch using BJH model are shown in Fig.7b. Both the unsupported OMC membrane and OMC hollow fiber membrane possess a narrow peak centering at 4.33nm. As shown in Table 2, the unsupported OMC membrane has a BET surface area of 665 m^2/g and pore volume of 0.44 cm^3/g . Differently, the OMC hollow fiber membrane has a smaller surface area of $\sim 565m^2/g$ and pore volume of 0.34

cm³/g, which can be attributed to the presence of pyrolyzed PVDF UF membranes. The specific surface area and pore volume of OMC materials are comparable to those in literature reports¹².

3.3 Gas permeation properties

In order to evaluate the integrity and separation performance of the OMC hollow fiber membrane, five single-gas permeation tests were conducted at room temperature. From the permeance versus average pressure data (Fig.8a), it can be seen that the permeance of different gases were clearly independent of the feed pressure, indicating that the viscous flow does not contribute to the total permeation. This implies that the prepared OMC hollow fiber membrane is crack-free²⁸, which is in agreement with SEM observation.

Several research groups have reported on the single gas permeation properties of the OMC membranes supported on various substrates^{12,30,31}. After normalized by the thickness of OMC membrane, the permeance of N₂ through the OMC hollow fiber membrane is enhanced by at least 50% compared to that in supported OMC membranes. It is suggested that the OMC hollow fiber membrane with ordered mesopores and defect holes facilitates the nitrogen molecular diffusion compared to supported OMC membranes in previous reports.

The molecular weight dependency of gas permeance of the OMC hollow fiber membrane is plotted in Fig. 8b. The permeance of H₂, He, N₂, Ar, and CO₂ gases is linearly proportional to the inverse squared root of molecular weight. A good fit between the experimental data and the linear regression line passing through the origin was found. This behavior is a characteristic feature of gas transport by Knudsen mechanism⁴. Consequently, the gases through the membrane are governed by Knudsen diffusion, further indicating that the prepared OMC hollow fiber membrane is defect-free.

4. Conclusion

A new method to prepare novel OMC hollow fiber membrane by confined soft templating route has been demonstrated. Well-developed mesoporous structure with dominant pore diameters of 4.33 nm was observed for the prepared OMC hollow fiber membrane. Single gas tests indicate the diffusion of gases through the membrane is governed by Knudsen diffusion, which confirms the defect free characteristic of the obtained OMC hollow fiber membrane. High surface area/volume ratio provided by hollow fiber configuration, ordered mesostructure along with specific characteristic of carbon will hold great promise with regard to its application in nanofiltration, membrane reactors, chemical sensors, etc.

Acknowledgments

This work was financially supported by the National Natural Science Foundation of China (Grant No. 51278247). We acknowledge gratefully Professor Dongyuan Zhao for useful discussion and suggestion.

References

1. M. B. Shiflett, J. F. Pedrick, S. R. McLean, S. Subramoney, H. C. Foley, *Adv. Mater.*, 2000, **12**, 21.
2. J. N. Barsema, N. F. A. van der Vegt, G. H. Koops, M. Wessling, *Adv. Funct. Mater.*, 2005, **15**, 69.
3. T. A. Centeno, A. B. Fuertes, *Carbon*, 2000, **38**, 1067.
4. M. Yoshimune, T. Yamamoto, M. Nakaiwa, K. Haraya, *Carbon*, 2008, **46**, 1031.
5. R. Ryoo, S. H. Joo, S. Jun, *J. Phys. Chem. B*, 1999, **103**, 7743.
6. C. D. Liang, K. L. Hong, G. A. Guiochon, J. W. Mays, S. Dai, *Angew. Chem., Int. Ed.*, 2004, **43**, 5785.
7. C. D. Liang, S. Dai, *J. Am. Chem. Soc.*, 2006, **128**, 5316.
8. F. Zhang, D. Gu, T. Yu, F. Zhang, S. Xie, L. Zhang, Y. Deng, Y. Wan, B. Tu, D. Zhao, *J. Am. Chem. Soc.*, 2007, **129**, 7746.
9. Y. Meng, D. Gu, F. Zhang, Y. Shi, L. Cheng, D. Feng, Z. Wu, Z. Chen, Y. Wan, A. Stein, D. Zhao, *Chem. Mater.*, 2006, **18**, 4447.
10. B. Platschek, A. Keilbach, T. Bein, *Adv. Mater.*, 2011, **23**, 2395.
11. J. Schuster, A. Keilbach, R. Koehn, M. Doeblinger, T. Doerfler, T. Dennenwaldt, T. Bein, *Chem. Eur. J.*, 2011, **17**, 9463.
12. S. Tanaka, N. Nakatani, A. Doi, Y. Miyake, *Carbon*, 2011, **49**, 3184.
13. L. Xu, M. Rungta, W. J. Koros, *J. Membr. Sci.*, 2011, **380**, 138.

14. X.He, M.B.Haegg, *Chem. Eng. J.*,2013, **215**, 440.
15. X.He, M.B.Hagg, *J. Membr. Sci.*,2012, **390**, 23.
- 16.X.He, J. A.Lie, E.Sheridan, M.B.Hagg,*In. Eng. Chem. Res.*,2011, **50**, 2080.
- 17.X.He, M.B.Hagg, *In. Eng. Chem. Res.*,2011,**50**, 8065.
- 18.X.He, M.B.Hagg,*J. Membr. Sci.*,2011, **378**, 1.
- 19.E. P.Favvas, G. E.Romanos, S. K.Papageorgiou, F. K. Katsaros,A. C.Mitropoulos, N. K.Kanellopoulos, *J. Membr. Sci.*,2011, **375**, 113.
- 20.R.Liu, Y.Shi, Y.Wan, Y.Meng, F.Zhang, D.Gu, Z.Chen, B.Tu, D.Zhao,*J. Am. Chem. Soc.*, 2006,**128**, 11652.
- 21.C.Huang, Y. B.Zhou, Y.Jin, X. F.Zhou, Z. M.Tang, X.Guo, S. B.Zhou, *J. Mater.Chem.*, 2011, **21**, 5660.
22. S. M.Lebedev, O. S.Gefle, S. N.Tkachenko, *J. Electrostat.*,2010,**68**, 122.
- 23.D.Zhao, J.Feng, Q.Huo, N.Melosh, G. H.Fredrickson, B. F.Chmelka,G. DStucky, *Science*,1998, **297**, 548.
- 24.S.Jun, S. H.Joo, R.Ryoo, M.Kruk, M.Jaroniec,Z.Liu, T.Ohsuna, O.Terasaki,*J. Am. Chem. Soc.*,2000, **122**, 10712.
- 25.K.X.Wang, P.Birjukovs,D.Erts, R.Phelan, M. A.Morris, H.S.Zhou, J. D.Holmes,*J. Mater.Chem.*, 2009,**19**, 1331.
- 26.K.X.Wang,W.H.Zhang,R.Phelan, M. A.Morris, J. D.Holmes, *J. Am. Chem. Soc.*,2007,**129**, 13388.
- 27.J.Li, Y.Hao, H.Li, M.Xia, X.Sun, L.Wang,*Microporous. Mesoporous. Mater.*,2009,**120**, 421.
- 28.H. P.Lin,S. T.Wong, C. Y.Mou, C. Y.Tang, *J. Phys. Chem.C*,2000,**104**, 8967.
- 29.J.Li, X.We, Y. S.Lin, D.Su,*J. Membr. Sci.*,2008,**312**, 186.
- 30.G.T.Qin, C. Wang, W.We, *Carbon* 2010, **48**(14),4197.
31. L.Li, C.W.Song, H.W.Jiang,J.S.Qiu, H.T.Wang,*J. Membr. Sci.*, 2014, **450**,469.

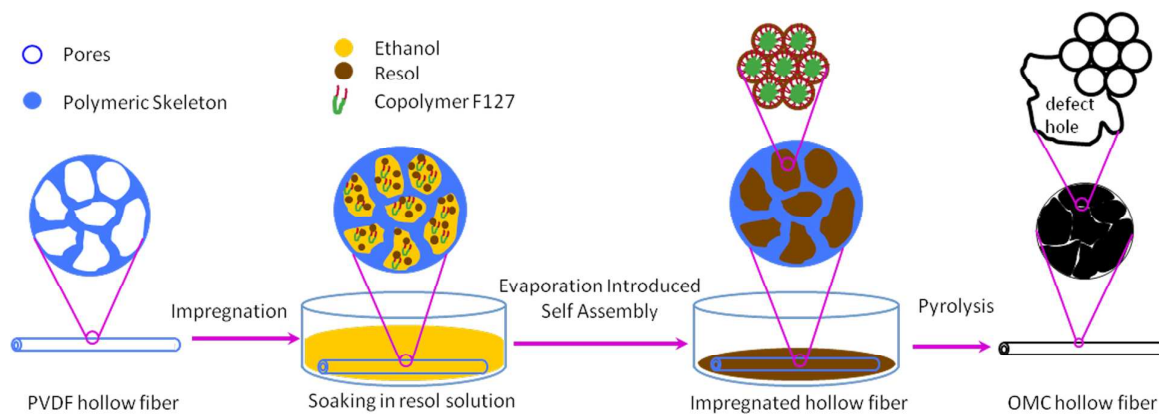


Fig.1 A scheme illustrating the confined soft templating approach

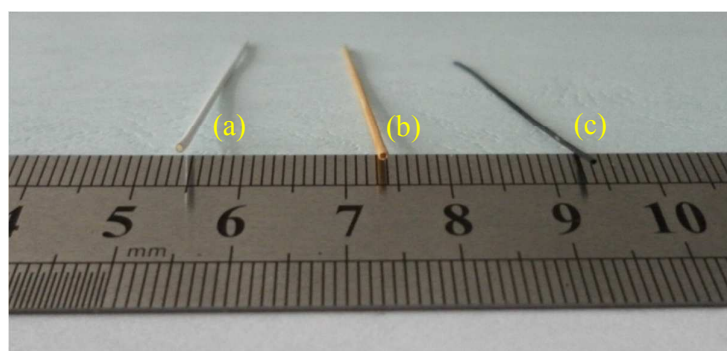


Fig. 2. Digital Photo of the PVDF hollow fiber membrane(a), impregnated hollow fiber membrane (b) and OMC hollow fiber membrane(c).

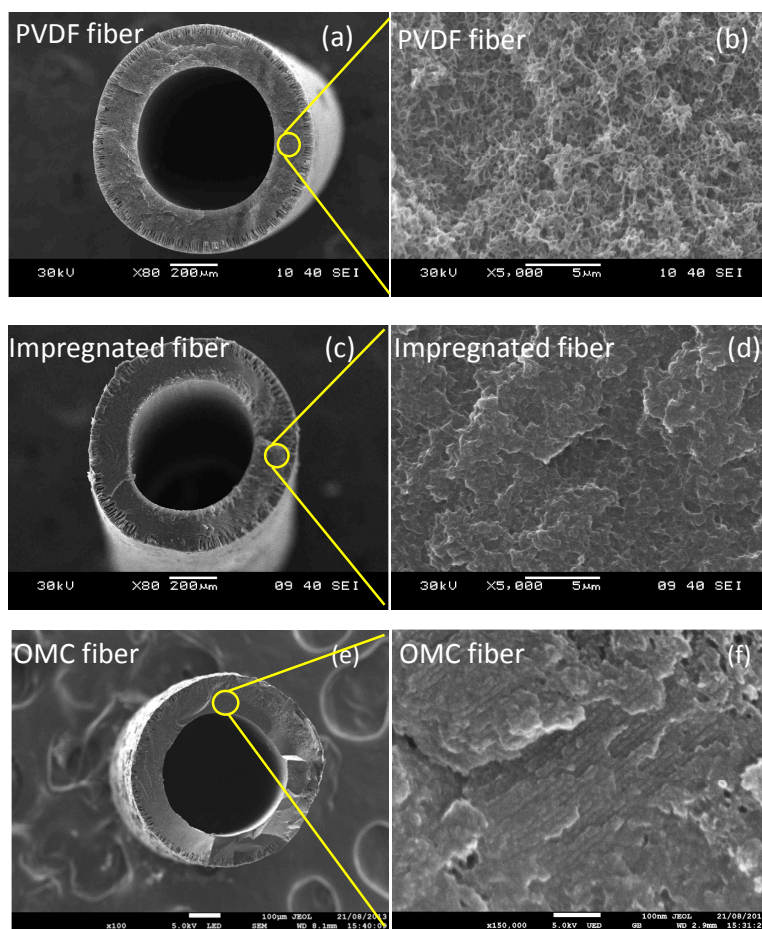


Fig.3 SEM images of the PVDF hollow fiber membranes (a,b), impregnated hollow fiber membrane (c,d) and FESEM images of OMC hollow fiber membranes (e,f).

Table 1 Dimension change of the samples

Sample ID	Length (cm)	Outer	Inner	Wall	Shrinkage (%)		
		diameter	diameter	thickness	Radial	Radial	Axial
		(μm)	(μm)	(μm)	direction(od)	direction(id)	direction
PVDF fiber	10.0	947	608	170	--	--	--
Impregnated fiber	9.2	893	548	173	5.7	9.9	8.0
OMC fiber	6.9	663	438	113	30.0	28.0	31.0

Note: od: outer diameter; id: inner diameter

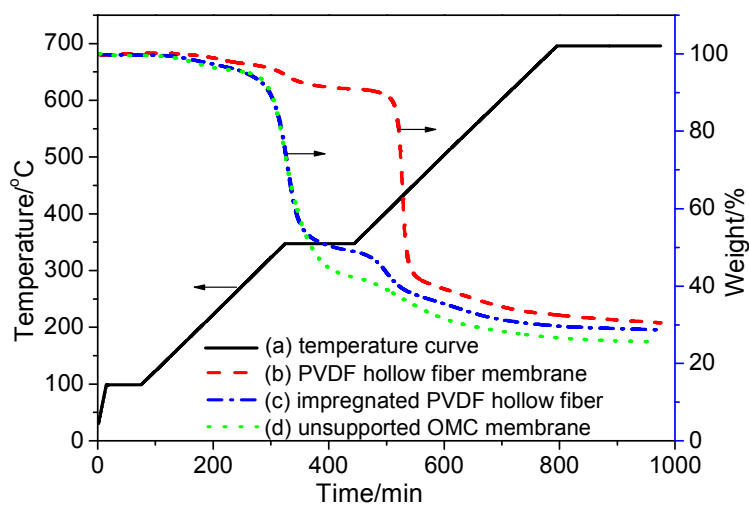


Fig. 4 Temperature curve (a) and weight loss profiles of the PVDF hollow fiber membrane (b), impregnated hollow fiber membrane (c), and unsupported OMC membrane (d) from TGA analysis.

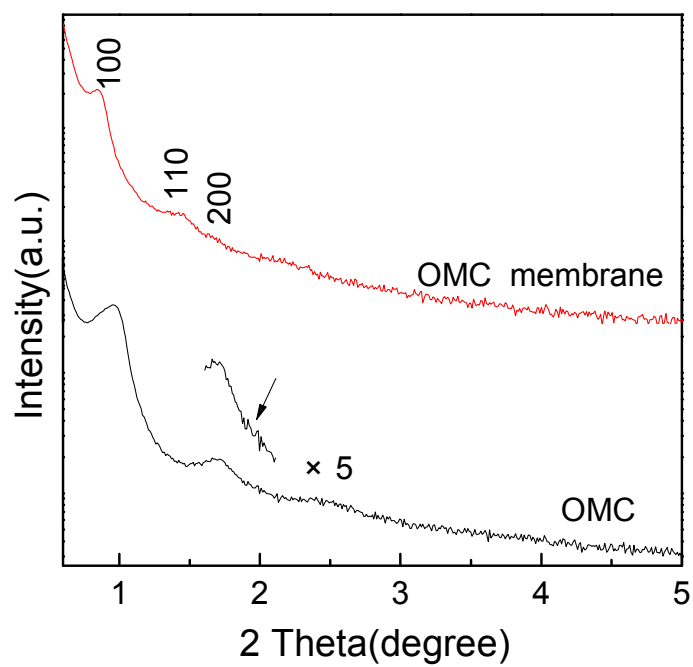


Fig. 5 Small-angle XRD patterns of the unsupported OMC membrane and OMC hollow fiber membrane.

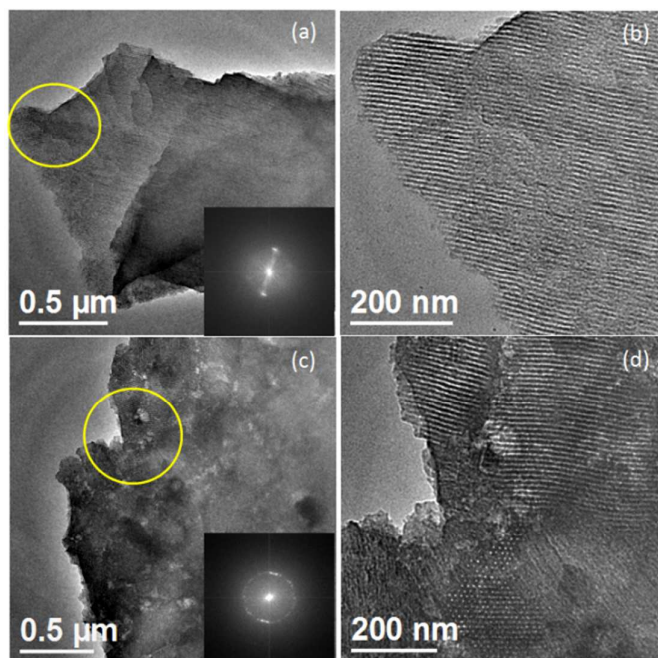


Fig. 6 TEM images of unsupported OMC membrane (a,b) and OMC hollow fiber membrane (c,d).

The insets are the corresponding FFT diffractograms.

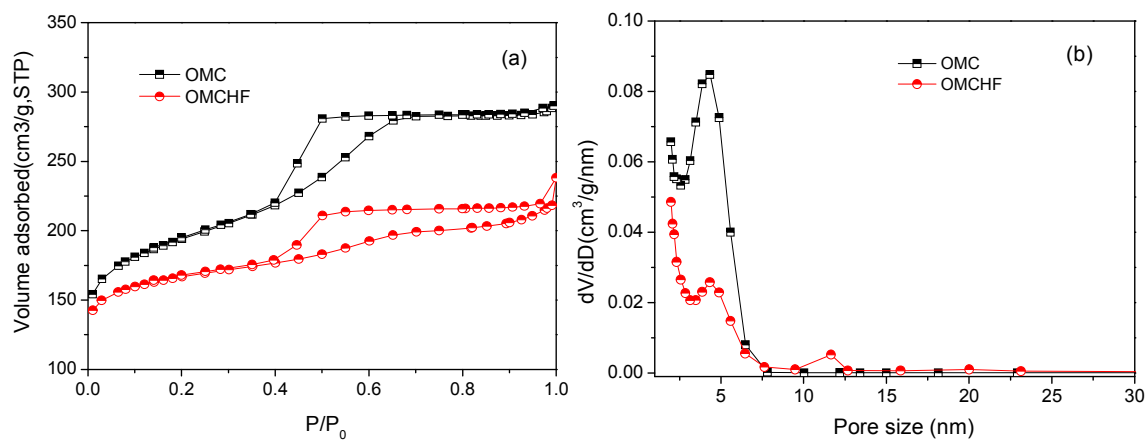


Fig. 7. (a) Nitrogen adsorption-desorption isotherms and (b) the pore size distribution of the unsupported OMC membrane and OMC hollow fiber membrane.

Table 2 Structural parameters of the unsupported OMC membrane and OMC hollow fiber

membrane				
Samples	$S_{\text{BET}}/\text{m}^2\text{g}^{-1}$	$V_t/\text{cm}^3\text{g}^{-1}$	a/nm	d/nm
OMC	665	0.44	10.73	4.33
OMC fiber	565	0.34	11.96	4.33

Note: V_t is total pore volume; a is Unit cell parameter, $a = 2d_{100}/\sqrt{3}$; d is the pore diameter.

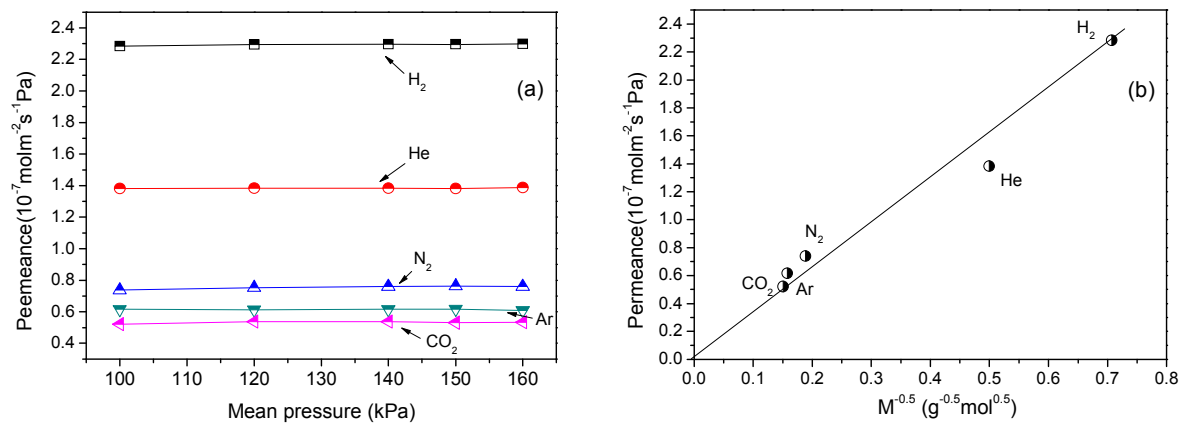


Fig.8. Different gases permeance (a) and dependency of permeance data through OMC hollow fiber membrane on the molecular weight (b).